



Cardiomyocyte specific overexpression of a 37 amino acid domain of regulator of G protein signalling 2 inhibits cardiac hypertrophy and improves function in response to pressure overload in mice



Katherine N. Lee^a, Xiangru Lu^a, Chau Nguyen^b, Qingping Feng^a, Peter Chidiac^{a,*}

^a Department of Physiology and Pharmacology, University of Western Ontario, London, ON, N6A5C1, Canada

^b School of Pharmacy, D'Youville College, Buffalo, New York 14201, USA

ARTICLE INFO

Article history:

Received 1 April 2016

Received in revised form 16 June 2017

Accepted 17 June 2017

Available online 19 June 2017

Keywords:

RGS2^{eb}

RGS2

Cardiac hypertrophy

Protein synthesis

Cardiac hypertrophy

ABSTRACT

Regulator of G protein signalling 2 (RGS2) is known to play a protective role in maladaptive cardiac hypertrophy and heart failure *via* its ability to inhibit G_q- and G_s- mediated GPCR signalling. We previously demonstrated that RGS2 can also inhibit protein translation and can thereby attenuate cell growth. This G protein-independent inhibitory effect has been mapped to a 37 amino acid domain (RGS2^{eb}) within RGS2 that binds to eukaryotic initiation factor 2B (eIF2B). When expressed in neonatal rat cardiomyocytes, RGS2^{eb} attenuates both protein synthesis and hypertrophy induced by G_q- and G_s- activating agents. In the current study, we investigated the potential cardioprotective role of RGS2^{eb} by determining whether RGS2^{eb} transgenic (RGS2^{eb} TG) mice with cardiomyocyte specific overexpression of RGS2^{eb} show resistance to the development of hypertrophy in comparison to wild-type (WT) controls. Using transverse aortic constriction (TAC) in a pressure-overload hypertrophy model, we demonstrated that cardiac hypertrophy was inhibited in RGS2^{eb} TG mice compared to WT controls following four weeks of TAC. Expression of the hypertrophic markers atrial natriuretic peptide (ANP) and β-myosin heavy chain (MHC-β) was also reduced in RGS2^{eb} TG compared to WT TAC animals. Furthermore, cardiac function in RGS2^{eb} TG TAC mice was significantly improved compared to WT TAC mice. Notably, cardiomyocyte cell size was significantly decreased in TG compared to WT TAC mice. These results suggest that RGS2 may limit pathological cardiac hypertrophy at least in part *via* the function of its eIF2B-binding domain.

© 2017 The Authors. Published by Elsevier Ltd. This is an open access article under the CC BY-NC-ND license (<http://creativecommons.org/licenses/by-nc-nd/4.0/>).

1. Introduction

Pathological cardiac hypertrophy is a maladaptive growth response of the heart to a variety of disease stimuli. Induced by factors such as hypertension or valvular diseases, prolonged pathological hypertrophy has been associated with an increased risk of sudden death, as well as myocardial infarctions and arrhythmias [1–3]. Moreover, maladaptive hypertrophy is a major risk factor for heart failure [3]. Given the high mortality rates following heart failure diagnoses and the current lack of a cure, reducing risk factors such as pathological cardiac hypertrophy may prove therapeutically beneficial.

G protein-coupled receptors (GPCRs) which signal *via* heterotrimeric G_α_q and G_α_s proteins are well established as critical players in the induction of pathological hypertrophy [3–5]. Clinically

effective treatments for heart failure, such as angiotensin II converting enzyme (ACE) inhibitors and beta-adrenergic receptor antagonists, demonstrate the effectiveness of targeting G_q- and G_s- coupled receptors [6]. However, the effectiveness of these drugs is limited to slowing, rather than reversing, the progression of heart failure. Regulator of G protein signalling 2 (RGS2) is a GTPase accelerating protein (GAP) found ubiquitously throughout the body. RGS2 selectively inhibits G_q- and G_s-mediated signalling (some effects on G_{i/o} signalling have also been reported [7,8]), thus making it an important target in the study of cardiovascular disease [9–11]. Studies *in vivo* and in cardiomyocytes have shown that hypertrophy caused by prolonged G_q-coupled receptor stimulation, such as that induced by phenylephrine, can be blocked by the overexpression of RGS2 [12,13]. A similar effect has been seen against G_s-mediated cardiomyocyte hypertrophy induced by isoproterenol [14]. These observations suggest that RGS2 plays an important role in the regulation of hypertrophy; this has been further demonstrated in knockout animal studies. In RGS2 null mice, experimentally induced pressure overload causes marked hypertrophy, heart failure, and death, as well as increased expression of cardiac fetal genes [15]. Thus, RGS2 would appear to be an essential element in the prevention of pathological cardiac hypertrophy.

Abbreviations: (eIF2), eukaryotic initiation factor 2; (eIF2B), eukaryotic initiation factor 2B; (GPCRs), G protein-coupled receptors; (HWT/BWT), heart weight/body weight; (LV), left ventricle; (RGS2), regulator of G protein signalling 2; (RGS2^{eb}), RGS2-eIF2B binding domain; (TG), transgenic; (TAC), Transverse aortic constriction; (WT), wildtype.

* Corresponding author at: Department of Physiology and Pharmacology, Medical Sciences Building, University of Western Ontario, London, ON, N6A5C1, Canada.

E-mail address: peter.chidiac@schulich.uwo.ca (P. Chidiac).

While the G protein inhibitory effects of RGS2 are well established, studies have also shown that RGS2 can bind to and regulate other targets, including TRPV6 calcium channels and tubulin [16–18]. We have previously shown that RGS2 can bind to the epsilon subunit of eukaryotic initiation factor 2B (eIF2B), a component of the rate-limiting step of the initiation of mRNA translation [19]. By interacting with eIF2B, RGS2 limits GDP dissociation on eukaryotic initiation factor 2 (eIF2), which ultimately leads to the attenuation of *de novo* protein synthesis. This property of RGS2 has been mapped to a 37 amino acid domain (residues 79–115) termed RGS2^{eb}, that is homologous to a region in the beta subunit of eIF2 [19].

Since the heart is considered to be a post-mitotic organ [20], hypertrophic growth is thought to be dependent on the enlargement of a pre-existing cardiomyocyte population rather than cell division [21]. Therefore, regardless of the initial stimuli and receptors involved, all hypertrophic signals will ultimately result in increased mRNA translation and *de novo* protein synthesis. Our previous studies have shown that RGS2^{eb} expression in cultured neonatal cardiomyocytes is able to inhibit both protein synthesis and agonist induced hypertrophy at levels comparable to full-length RGS2 [22]. Based on these previous findings, we hypothesized that the *in vivo* expression of RGS2^{eb} in the murine heart could attenuate the development of pathological cardiac hypertrophy. To determine whether RGS2^{eb} could act as an *in vivo* anti-hypertrophic agent, we developed a line of transgenic mice with cardiomyocyte-specific overexpression of RGS2^{eb}, and used transverse aortic constriction (TAC) to induce pressure overload on the heart. Here we report that following 4 weeks of aortic constriction, RGS2^{eb} transgenic mice were protected against pressure overload-induced cardiac hypertrophy, and also were able to maintain heart function at significantly improved levels compared to WT TAC mice. Moreover, reactivation of the “fetal gene program”, an indicator of hypertrophy and heart failure, was suppressed. Notably, cardiomyocyte size was decreased in RGS2^{eb} TG compared to WT TAC controls, further supporting our earlier *in vitro* studies which showed RGS2^{eb} inhibition of *de novo* protein synthesis. Together, these findings suggest that in addition to its G-protein inhibitory actions, the RGS2^{eb} region may be contributing to the cardioprotective effects of full-length RGS2 *in vivo* via the inhibition of *de novo* protein synthesis.

2. Materials and methods

2.1. Generation of myosin heavy chain promoter (MHC) - RGS2^{eb} transgenic mice

The RGS2^{eb} gene was targeted to the heart using the mouse α -MHC promoter (kindly provided by Jeffrey Robbins, Cincinnati Children's Hospital Medical Center) [23]. Transgenic mice were generated in the FVB background (London Regional Transgenic and Gene Targeting Facility) and identified by polymerase chain reaction (PCR). Briefly, ear biopsies were taken from three-week old mice and purified for genomic DNA using the QIAquick PCR purification kit (Qiagen). PCR was performed using DreamTaq Green PCR Master Mix (Thermo Scientific). Primers for detection of transgenic mice (CTGCTAGCCAGCAAATATGGTC forward, CCTACAGGTTGTCTTCCCAACT reverse) and control primers for endogenous RGS2 expression (CCGAGTCTGTGAAGAAAACATTG forward, ATGCTACATGAGACCAGGAGTCCC reverse) were designed using the OligoPerfect Designer (ThermoFisher), OligoCalc [24], and Primer-BLAST (NCBI) programs, resulting in a 293 bp and 342 bp fragment, respectively. RGS2^{eb} TG transgenic mice were back-crossed with C57Bl/6 mice (Charles River) for at least seven generations before animal experiments were performed. Animals were maintained in accordance with the Institute of Laboratory Animal Research Guide for the Care and Use of Laboratory Animals. These studies were approved by the Council on Animal Care at the University of Western Ontario, and complied with the guidelines of the Canadian Council on Animal Care.

2.2. Transverse aortic constriction (TAC)

TAC was used to induce pressure overload on the hearts of 12 week old male C57Bl/6 wild-type mice and RGS2^{eb} TG littermates. Mice were anaesthetized with a ketamine (50 mg/kg) and xylazine (12.5 mg/kg) cocktail intramuscularly, intubated, and ventilated with a respirator (SAR-830, CWE, Ardmore, PA, USA). To access the chest cavity, thoracotomy was performed at the second intercostal space under a surgical microscope [25]. A 6–0 silk suture was placed between the brachiocephalic and left carotid arteries. Two knots were tied against a 25-gauge blunt needle placed parallel to the transverse aorta. The needle was removed immediately after the second tied knot followed by closure of the chest. Control WT and RGS2^{eb} TG mice were subjected to sham operations without aortic constriction.

2.3. Assessment of cardiac function

Hemodynamic measurements were performed as previously described [26,27]: four weeks post-surgery, mice were again anaesthetized with a ketamine and xylazine cocktail and ventilated. A Millar micro-tip pressure catheter was inserted into the left carotid artery to assess carotid artery pressure, followed by removal of the catheter and insertion into the right carotid artery for pressure readings, and then advanced into the left ventricle (LV) to measure LV pressures, volumes, and heart rate at steady state and during transient preload reduction via mechanical occlusion of the inferior vena cava. All data were recorded using a PowerLab data acquisition system and analyzed by LabChart 7.0 (ADInstruments) and PVAN 3.4 software (Millar).

2.4. Heart weight/body weight ratios

Upon completion of hemodynamic recordings, mice were immediately euthanized via a 10% KCl injection into the left jugular vein to ensure cardiac arrest in the diastolic state. Hearts were excised, weighed after removal of the atria, then cut transversely into three equal sections, with the middle section reserved for histological analysis, and the remaining tissue sections stored at -80°C for subsequent RNA isolation.

2.5. Histological analysis

Heart samples were fixed in 4% paraformaldehyde overnight at 4°C , dehydrated, and paraffin embedded. Samples were sectioned into $5\ \mu\text{m}$ thick slices with a Leica RM2255 microtome, mounted onto positively charged slides, and then stained with haematoxylin and eosin. Images of left ventricles were captured at $400\times$ magnification with a Zeiss Observer D1 microscope using AxioVision 4.7 software (Zeiss) for cardiomyocyte size measurements and immunohistochemical imaging; images of the LV for wall thickness measurements were captured at $100\times$ magnification.

2.6. Cardiomyocyte cell size and LV wall thickness

Haematoxylin and eosin stained tissue sections were used to determine left ventricular cardiomyocyte cell size and wall thickness of LV free walls and septum. The size of an individual cardiomyocyte was determined by measuring its cross-sectional area. All cardiomyocytes with a well-defined border were manually outlined and then filled in the open source GNU Image Manipulation Program (GIMP). Images were then opened in the image processing program ImageJ and analyzed after setting the threshold. Cardiomyocytes with a circularity ratio of ≥ 1.2 were excluded to eliminate cells sectioned tangentially [28]. Areas of at least 33 cells per animal were measured, and were scored blind to surgeries and strain.

Heart wall thickness of the LV free wall was measured using AxioVision 4.7 software (Zeiss) in three distinct areas within and between the

anterior and posterior regions of the free wall; three measurements were taken from each area for a total of 9 averaged measurements per sample. For the septal wall, single measurements were taken from three distinct areas of the wall and averaged for each sample.

2.7. Immunohistochemistry

Immunohistochemical staining was performed on 5 μ m thick paraffin heart sections. Samples underwent a deparaffinisation process and antigen retrieval was carried out in sodium citrate buffer (pH 6.0) at 92 °C using a BP-111 laboratory microwave (Microwave Research and Applications). Sections were incubated with primary antibody anti-6X His tag-ChIP Grade (Abcam) overnight followed by biotinylated secondary antibody, and signal was detected using avidin-biotin complex (ImmunoCruz ABC staining kit, Santa Cruz). Diaminobenzidine (DAB) substrate solution was used for antigen visualization with haematoxylin as a counterstain. Following staining, the LV free wall was imaged in three distinct locations within and between the anterior and posterior walls. Slides were imaged at 400 \times magnification with a Zeiss Observer D1 microscope using AxioVision 4.7 software. To ensure accurate comparisons of antigen visualization, sections from WT and RGS2^{eb} TG genotypes were stained simultaneously and all images were captured using the same microscopic parameters.

2.8. Dot blotting

Using mechanical disruption (Sonic Dismembrator Model 100, Fisher Scientific), LV heart and kidney tissues from RGS2^{eb} TG and WT mice were lysed in 20 mM, pH 7.5 Tris-HCl buffer containing cOmplete Mini protease inhibitor cocktail (Sigma). Samples were centrifuged at 100,000g for 1 h at 4 °C in an Optima TLX micro-ultracentrifuge (Beckman Coulter), and supernatants were kept for experiments. Following protein concentration determination by Bradford assay, equal amounts of sample protein were spotted directly on to Amersham Protran 0.2 μ m pore size nitrocellulose membrane (GE Healthcare Life Sciences). Purified histidine-tagged RGS-16 (His-RGS16) was also dotted on to membranes to serve as a positive control. Dried membranes were blocked in 5% milk-TBST, followed by overnight incubation in 1:2000 ChIP grade anti-6X Histidine primary antibody (Abcam) and then 1:5000 goat anti-rabbit secondary antibody HRP conjugate (Invitrogen). Signal was detected using SuperSignal West Pico chemiluminescent substrate (Thermo Fisher Scientific) and imaged with the Versadoc MP 5000 system and Quantity One software (Bio-Rad).

2.9. Quantitative reverse transcription PCR

Total RNA was isolated from heart tissue using the TriZol (Invitrogen) extraction method. Reverse transcription reaction was performed using the High-Capacity cDNA Reverse Transcription Kit with RNase Inhibitor (Invitrogen). SensiFAST SYBR No-ROX Kit mastermix (FroggaBio) was used for real-time thermal cycling. Primers for RGS2 (TGGGATTATGTGGCCTTAGC forward, AAGAACGTCAACACCCTTGC reverse), hGH (TGGGAAGACAACCTGTAGGG forward, AATCGCTTGAACCCAGGAG reverse), β -MHC (CTGAGACGGAGAATGGCAAGAC forward, ACTTGTAGGGGTTGACGGTGAC reverse), ANP (ATTCTGAGACGTCCCTTT forward, CATTCCATCCACAGCTCCT reverse), and BNP (TGGGAATTAGCCATGTGAGAG forward, TTTGGGTGTTCTTTGTGAGG reverse) were designed using the OligoPerfect Designer (ThermoFisher), OligoCalc [24] and Primer-BLAST (NCBI) programs. Samples were amplified for 35 cycles using the Eppendorf Mastercycler Realplex Real-Time PCR machine. The mRNA quantity for each gene of interest was determined using standard curve analysis and normalized to 28S ribosomal expression.

2.10. Statistical analysis

All data were analyzed using GraphPad Prism 6.01 (GraphPad). All statistical analyses were performed using two-way ANOVA followed by Bonferroni post-tests and presented as mean \pm SEM. Differences were considered significant at $P < 0.05$.

3. Results

3.1. Generation of transgenic mice with cardiomyocyte specific expression of RGS2^{eb}

We previously demonstrated that the *in vitro* expression of RGS2^{eb} was sufficient to inhibit drug-induced hypertrophy in isolated neonatal rat cardiomyocytes [22]. To elucidate the potential *in vivo* protective role of RGS2^{eb}, we developed a novel strain of transgenic mice with targeted myocardial overexpression of polyhistidine-tagged RGS2^{eb} under the control of the α -myosin heavy chain promoter (Fig. 1A). Genotyping with primers for a portion of the hGH polyA region, which was only present in the transgenic sequence of RGS2^{eb} mice, was used to differentiate between RGS2^{eb} TG and wildtype mice. Both RGS2^{eb} TG and WT controls displayed a band at 342 bp indicating the presence of endogenous full-length RGS2 (Fig. 1B); only RGS2^{eb} transgenic mice displayed an additional 293 bp band, which indicated the presence of the hGH poly A region. Due to the short length of the RGS2^{eb} transgene and difficulty in immunoblotting [22], immunohistochemical staining, qPCR for RGS2 and the human growth hormone (hGH), as well as dot blot visualization for the polyhistidine tag were used to confirm expression of the RGS2^{eb} transgene. Following DAB visualization, WT mice showed an absence of staining for polyhistidine, whereas RGS2^{eb} TG mice displayed positive antigen staining (Fig. 1C). Endogenous RGS2 appears to be decreased in both WT and RGS2^{eb} TG mice following TAC (Fig. 1D), which has been previously demonstrated [29], however this was not statistically significant. Expression of a region of hGH, which should only be present in transgenic mice, is significantly higher in RGS2^{eb} TG mice than in WT animals (Fig. 1E). In addition, LV heart tissues from RGS2^{eb} TG mice showed positive signals for polyhistidine when visualized on dot blots, whereas no signal was detected in non-cardiac tissue (*i.e.* kidney) and LV samples from WT mice (Fig. 1F). Together, these results indicate successful generation of transgenic mice with cardiomyocyte specific overexpression of RGS2^{eb}.

3.2. Improved cardiac function in RGS2^{eb} transgenic mice following pressure overload

Transverse aortic constriction (TAC) was used to induce experimental pressure overload on wildtype and RGS2^{eb} TG hearts. Following 4 weeks of constriction, systolic pressure was significantly increased in the right carotid artery, but significantly reduced downstream of the TAC site in the left carotid artery in both WT and RGS2^{eb} TG mice (Fig. 2A and B). This resulted in a 61 \pm 10 mm Hg difference in maximal systolic pressure between the left and right carotid arteries of WT sham and TAC mice, and a 62 \pm 9 mm Hg difference between RGS2^{eb} TG sham and TAC mice (Fig. 2C). These data, as well as summary hemodynamic parameters in Table 1, confirm that pressure overload had indeed been induced upon TAC hearts. Increased vascular resistance was reflected by significantly higher end-systolic pressures in TAC mice; increased afterload as well as cardiac dilation or hypertrophy in TAC mice was also indicated by significant increases in the end systolic and end diastolic volumes (Table 1). Heart rate under anaesthesia was maintained at similar levels in all surgery groups (Fig. 2D).

Following pressure-volume loop analysis, RGS2^{eb} TG mice demonstrated improved cardiac function as measured by multiple systolic and diastolic indices. Summary data for contractility and relaxation (maximal elastance, ejection fraction, left ventricular systolic pressure, arterial elastance, LV + dP/dt, LV - dP/dt, and time constant tau) are

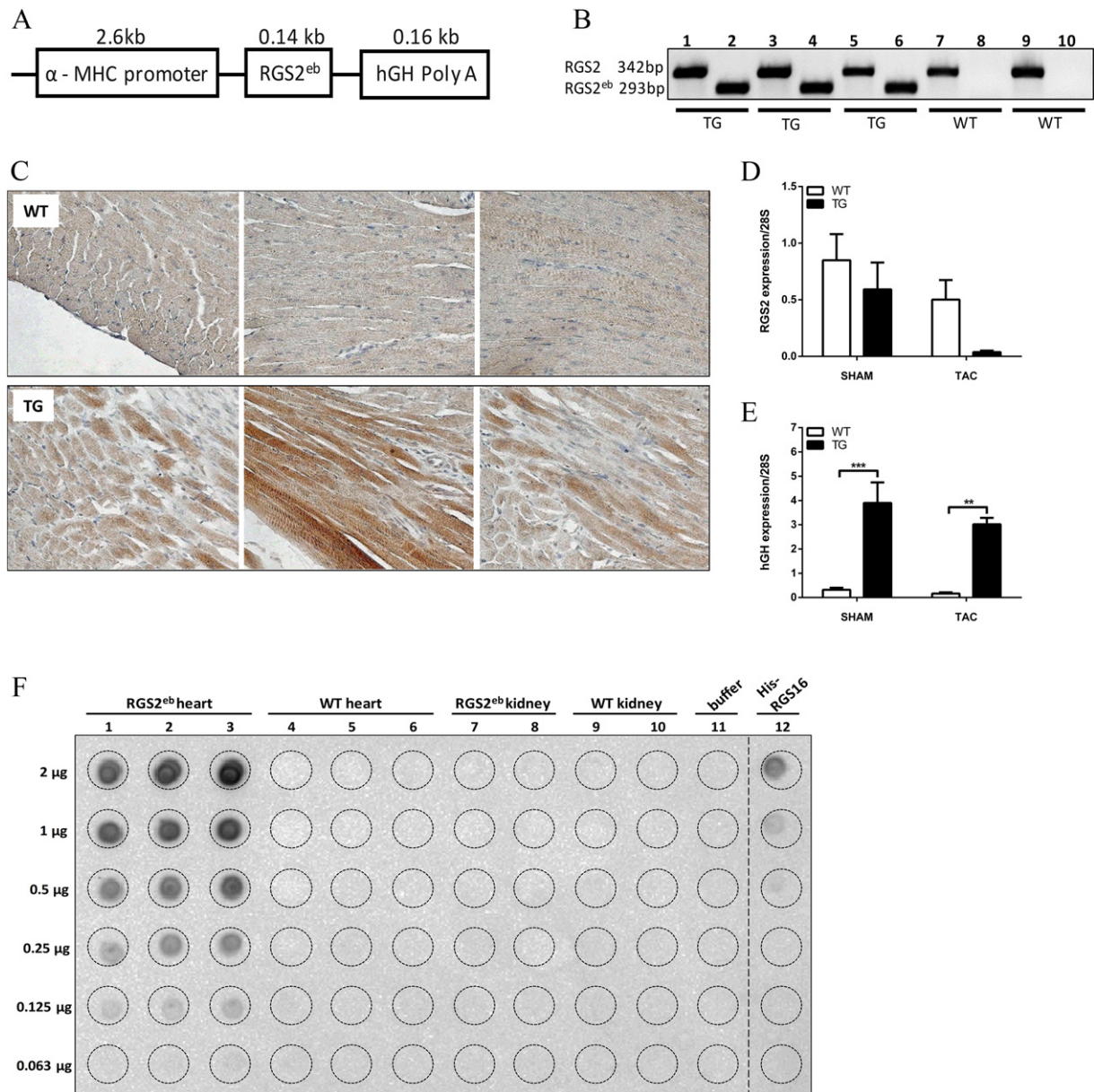


Fig. 1. Generation of transgenic mice with cardiomyocyte specific expression of RGS2^{eb}. (A) Construct used for the generation of mice with cardiomyocyte-specific overexpression of RGS2^{eb} under the control of α -myosin heavy chain. (B) Genotyping for a region which includes the hGH PolyA sequence results in a positive band for RGS2^{eb} TG mice and the absence of a band in WT controls (lanes 8 and 10), while genotyping for endogenous RGS2 resulted in bands for both RGS2^{eb} TG and WT controls (lanes 1, 3, 5, 7, and 9). (C) Representative immunostaining in the left ventricle of WT mice shows an absence of polyhistidine staining, whereas RGS2^{eb} TG mice display positive immunostaining for polyhistidine. (D) RGS2 and (E) hGH qPCR expression in WT and RGS2^{eb} TG mice following sham or TAC surgery. (F) Signal for polyhistidine was only detected in the LV tissue of RGS2^{eb} TG mice and His-RGS16 positive controls, with no signal detected in non-cardiac tissue or WT mice. Data represent means \pm SEM, $n = 5$ –6 per group. ** $P < 0.01$, and *** $P < 0.001$ using two-way ANOVA with Bonferroni's *post hoc* test for multiple comparisons.

provided in Fig. 3. Notably, Millar catheter measurements of the maximal and minimal rates of pressure change in the left ventricle (LV +dP/dt and LV -dP/dt, respectively), which are important indices of cardiac contractility, were significantly greater in RGS2^{eb} TG TAC mice compared to WT TAC counterparts (Fig. 3F and G). In addition, WT TAC mice showed significant increases in the Tau relaxation constant (Fig. 3H), indicating impairment of active properties of diastolic relaxation [30]. These data suggest that the functional deficit in RGS2^{eb} TG mice following 4 weeks of TAC is reduced in comparison to WT TAC animals.

3.3. Cardiac hypertrophy is inhibited in RGS2^{eb} transgenic mice following pressure overload

Following 4 weeks of TAC, heart weight/body weight (HWT/BWT) ratios, LV and septal wall thickness, and the cross-sectional

areas of cardiomyocytes were used to evaluate the development of cardiac hypertrophy. Although WT TAC mice developed significant cardiac hypertrophy (as measured by HWT/BWT) compared to sham controls, RGS2^{eb} TG mice displayed limited hypertrophic growth compared to WT TAC animals (Fig. 4A). Some hypertrophy does still appear to have occurred, as both WT and RGS2^{eb} TG mice exhibited significantly increased LV free wall thickness compared to corresponding sham controls (Fig. 4B, 4F and 4G); Septal wall thickness was not significantly changed in TAC surgery groups compared to sham controls (Fig. 4C). In addition, RGS2^{eb} TG TAC mice did not show marked changes in LV free wall cardiomyocyte size compared to TG sham controls, and were significantly smaller in size than cardiomyocytes from WT TAC mice (Fig. 4D and H (representative)). No changes were observed in measured cardiomyocytes from the septal wall (Fig. 4E). These data suggest that RGS2^{eb} may confer a

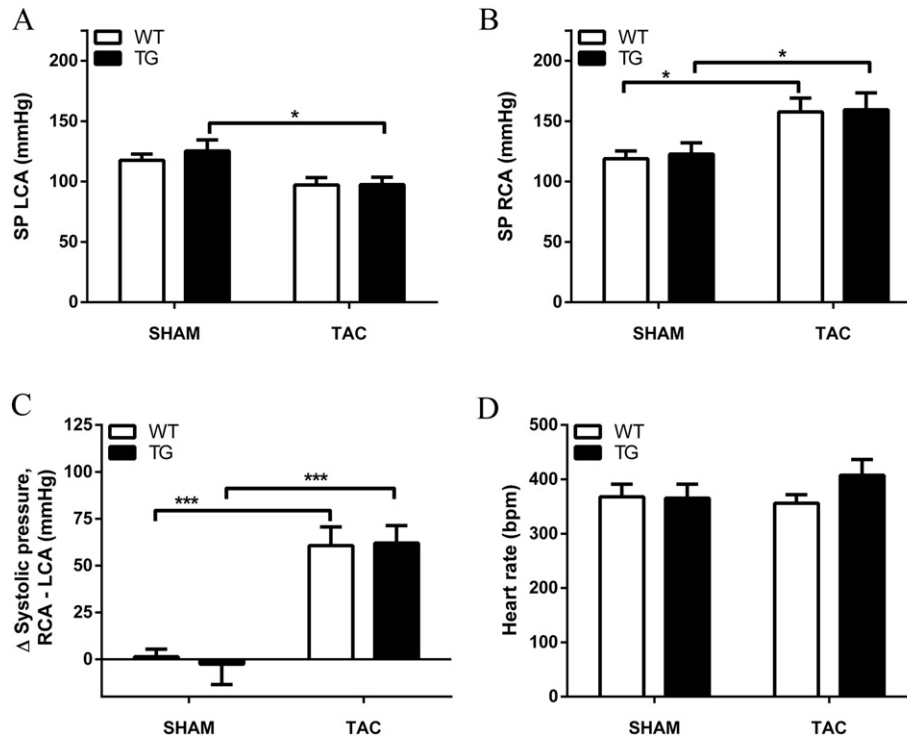


Fig. 2. Pressure overload model of transverse aortic constriction. (A) Following 4 weeks of aortic constriction between the left and right carotid arteries, systolic pressure in the LCA was reduced while (B) systolic pressure in the RCA was significantly increased. (C) Change in systolic pressure between the RCA and LCA following 4 weeks TAC was significantly increased in both WT and RGS2^{eb} TG mice. (D) Heart rate remained at similar levels for all experimental and genotype groups. Data represent means \pm SEM, n = 7–9 per group. * $P < 0.05$ and *** $P < 0.001$ using two-way ANOVA with Bonferroni's *post hoc* test for multiple comparisons.

protective effect in cardiomyocytes against pressure-induced cardiomyocyte hypertrophy.

3.4. Expression of cardiac hypertrophy markers is suppressed in RGS2^{eb} transgenic mice

Induction of “fetal” cardiac genes is often a common feature in animal models of pathological hypertrophy and heart failure [31,32]. RNA was isolated from left ventricular tissue after 4 weeks of TAC or sham surgery, and qPCR was performed to determine expression levels of β -myosin heavy chain (β -MHC), atrial natriuretic peptide (ANP), and brain natriuretic peptide (BNP). WT mice which underwent TAC showed significantly increased levels of both β -MHC and ANP compared to sham controls (Fig. 5A and B). In contrast, β -MHC and ANP expression in RGS2^{eb} TG mice after TAC was comparable to sham levels (Fig. 5A and 5B). BNP expression demonstrated a similar trend to that

seen with β -MHC and ANP, but this did not attain statistical significance between RGS2^{eb} TG and WT mice after TAC (Fig. 5C). Since the expression of fetal cardiac genes is postulated to be indicator of cardiac dysfunction, the absence of elevated levels in RGS2^{eb} TG mice after TAC suggests that the presence of RGS2^{eb} is cardioprotective in a pressure overload model of cardiac hypertrophy.

4. Discussion

In order for maladaptive cardiac hypertrophy to occur, individual cardiomyocytes must increase in size; such growth requires increased global protein synthesis, the rate of which is controlled primarily at the initiation level [33]. Of particular importance is the heterotrimeric initiation factor eIF2, which is activated by the heteropentameric protein eIF2B [34]. Notably, eIF2B has been shown to play a critical role in the development of β -adrenergic receptor induced hypertrophy in cultured cardiomyocytes [35]. A major role for eIF2B ϵ in controlling cell size is also evident from its regulation by glycogen synthase kinase 3 β (GSK3 β), which constitutively phosphorylates eIF2B ϵ at serine 540 in intact cells, thereby inhibiting its GEF activity by up to 80% [36]. In a cultured cardiomyocyte model, overexpression of a mutant eIF2B ϵ which could not be phosphorylated by GSK3 β increased cell size and abolished the antihypertrophic effects of GSK3 β , suggesting that eIF2B ϵ is a direct mediator of cardiac myocyte hypertrophy [35]. Importantly, further expression of a dominant-negative mutant of eIF2B ϵ inhibited isoproterenol-induced cardiac hypertrophy, indicating the critical role of eIF2B ϵ in protein synthesis and cell growth [35]. We have previously shown that the cellular effects of eIF2B ϵ are blocked by RGS2^{eb} as well as by full length RGS2 [14,22]. The goal of the present study was to determine whether the ability of RGS2 to inhibit protein synthesis and cardiomyocyte growth *in vitro* could be extended to an animal model of pathological cardiac hypertrophy. We therefore developed a mouse line with cardiomyocyte specific expression of RGS2^{eb}, and examined the functional, histological, and biochemical consequences of experimental

Table 1

Hemodynamic parameters in 4 week sham and TAC mice. Data represent means \pm SEM ** $P < 0.05$ and *** $P < 0.001$ vs. sham controls using two-way ANOVA with Bonferroni's *post hoc* test for multiple comparisons.

	SHAM		TAC	
	WT	TG	WT	TG
n	7–13	6–13	6–10	6–9
BWT (g)	29.3 \pm 1.0	30.7 \pm 1.0	30.1 \pm 0.6	28.1 \pm 1.0
ESP (mmHg)	98.2 \pm 6.9	73.3 \pm 14	134.1 \pm 8.1*	144.2 \pm 11**
EDP (mmHg)	7.6 \pm 1.4	6.0 \pm 2.3	15.0 \pm 3.9	15.5 \pm 5.6
ESV (μ L)	18.4 \pm 4.4	16.7 \pm 0.5	37.0 \pm 5.9*	39.3 \pm 6.5*
EDV (μ L)	26.1 \pm 3.3	25.9 \pm 2.3	50.6 \pm 7.5*	51.4 \pm 6.2*
SV (μ L)	19.9 \pm 2.4	18.5 \pm 2.6	14.1 \pm 2.1	15.7 \pm 2.7
SW (mmHg \times μ L)	1456.9 \pm 207	1523.8 \pm 187	1661.9 \pm 207	1667.6 \pm 231
CO (μ L/min)	7112.3 \pm 947	6517.8 \pm 907	6713.6 \pm 596	8152.1 \pm 1098

BWT, body weight; ESP, end systolic pressure; EDP, end diastolic pressure; ESV, end stroke volume; EDV, end diastolic volume; SV, stroke volume; SW, stroke work; CO, cardiac output.

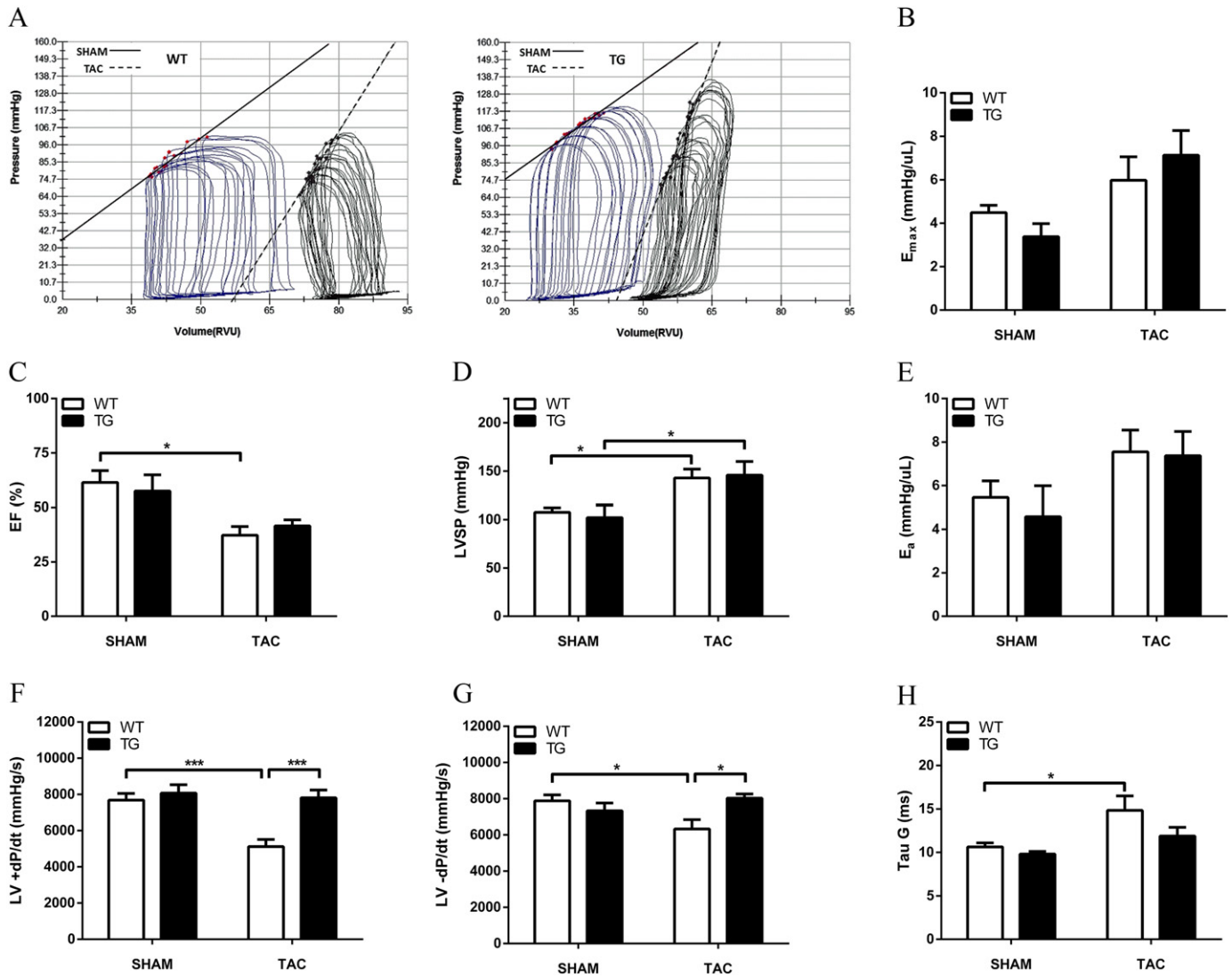


Fig. 3. Indices of systolic and diastolic function. (A) Representative PV loops during preload reduction by inferior vena cava occlusion in sham (solid lines) and 4 week TAC animals (dotted lines). (B) Slope of left upper relation (maximal elastance [E_{max}], reflected contractile function). (C) Ejection fraction was significantly reduced in WT but not RGS2^{eb} TG mice following pressure overload, while (D) LV systolic pressure (LVSP) was significantly elevated following TAC in both WT and RGS2^{eb} mice. (E) Effective arterial elastance (E_a ; an index of total ventricular afterload) was also increased following TAC. (F) LV +dP/dt and (G) -dP/dt were significantly improved in RGS2^{eb} mice following TAC, and (H) Tau relaxation time constant remained comparable to sham groups. Data represent means ± SEM, n = 6–9 per group. * $P < 0.05$ and *** $P < 0.001$ using two-way ANOVA with Bonferroni's *post hoc* test for multiple comparisons.

pressure overload in our transgenic mice and WT littermates. To the best of our knowledge, this is the first study to demonstrate that expression of a portion of RGS2, namely the RGS2^{eb} binding domain, can reduce pathogenic growth without adversely affecting *in vivo* cardiac function. Although a random insertion effect cannot be entirely excluded, expression of this transgene inhibited TAC-induced increases in heart weight/body weight ratio (Fig. 4A) and expression of hypertrophy-related gene markers (Fig. 5), as well as associated functional loss (Fig. 3). These results likely reflect the ability of RGS2^{eb} to inhibit protein synthesis *in vivo*, and the consequent suppression of the hypertrophic response and cardioprotective effects.

Using qPCR, immunohistochemistry and dot blotting methods, we have demonstrated the cardiac-specific expression of RGS2^{eb} in our transgenic mice (Fig. 1). However, due to the short length of the RGS2^{eb} transgene and difficulty in immunoblotting [22], a limitation of our study is our inability to fully demonstrate an eIF2B-RGS2^{eb} complex. Although RGS2^{eb} expression is associated with a decrease in cardiac hypertrophy and improved cardiac function, and our previous *in vitro* studies suggest that this is due to the inhibition of eIF2B, we cannot definitively attribute our *in vivo* observations to the direct inhibition of

protein synthesis, and thus cannot exclude other off target effects as the mechanism behind our observed cardioprotection.

Although LV free wall thickness was significantly increased in both WT and RGS2^{eb} TG mice following 4 weeks of TAC (Fig. 4B), HWT/BWT ratios indicated the development of significant TAC-associated cardiac hypertrophy in WT, but not RGS2^{eb} TG mice (Fig. 4A). Furthermore, measurements of cardiomyocyte cross-sectional area showed a corresponding increase in cell size for WT TAC but not RGS2^{eb} TG mice (Fig. 4D). These data suggest that *de novo* protein synthesis in response to pressure overload, and thus hypertrophy, is inhibited in RGS2^{eb} TG mice.

Our previous work showed that the adenoviral expression of RGS2^{eb} in neonatal ventricular myocytes was able to attenuate the expression of genetic markers of hypertrophy to a comparable extent as full-length RGS2 [22]. Thus, we examined whether RGS2^{eb} could also attenuate *in vivo* increases in the “fetal gene program”, a group of molecular markers associated with the hypertrophy phenotype, including β -MHC, ANP, and BNP [37–39]. Four weeks of aortic constriction induced an increase in the levels of β -MHC and ANP in WT mice (Fig. 5). These increases were completely abrogated in RGS2^{eb} TG animals. Reactivation of fetal

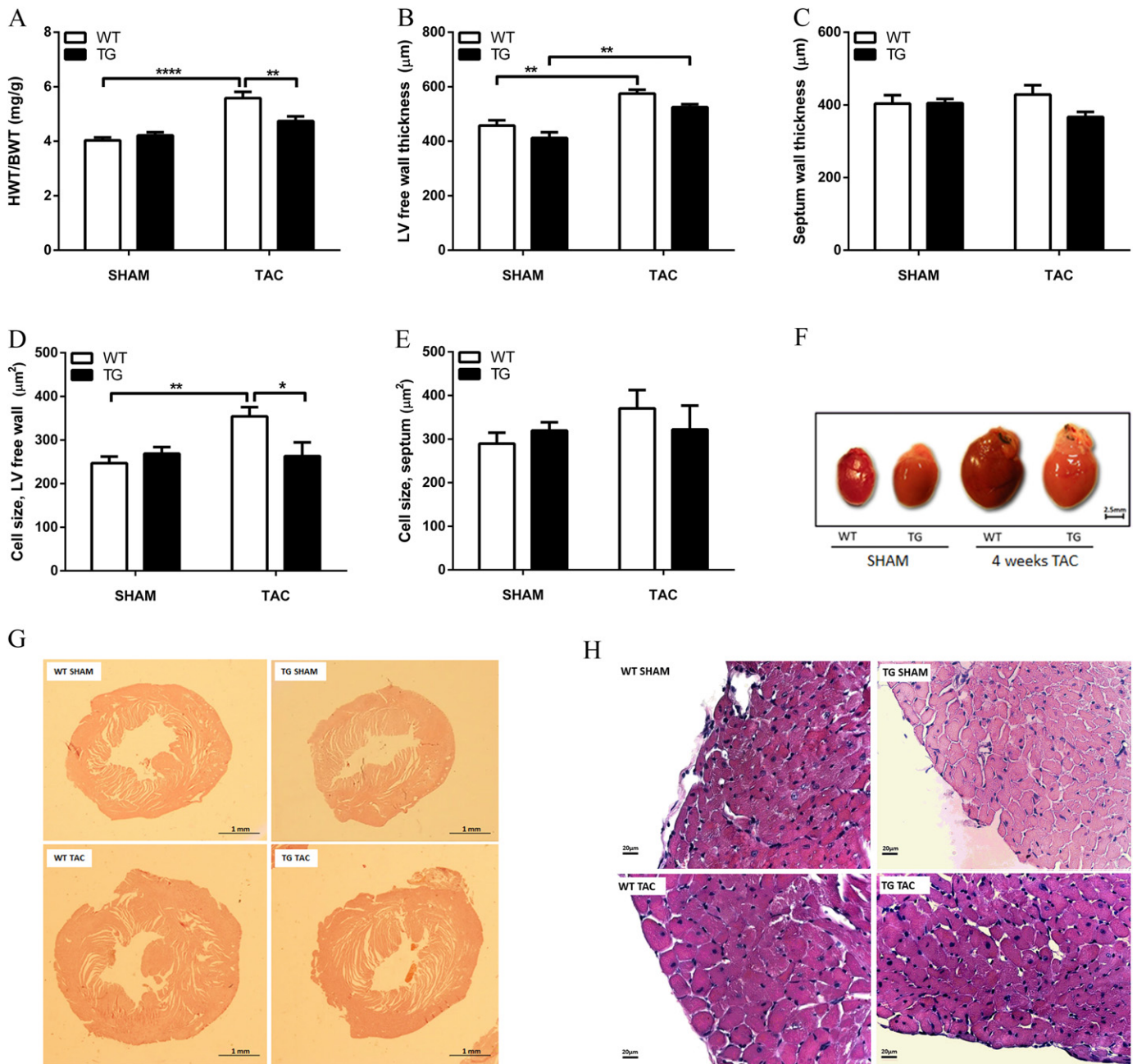


Fig. 4. Cardiac hypertrophy is inhibited in RGS2^{eb} transgenic mice following pressure overload. (A) After 4 weeks of aortic constriction, cardiac hypertrophy in RGS2^{eb} TG mice was significantly less than WT TAC. (B) LV free wall thickness was increased in both TAC groups; (C) septal wall thickness did not increase. (D) Cardiomyocyte size was significantly reduced in RGS2^{eb} TG mice compared to WT TAC in the LV free wall, with (E) no noticeable changes to size in the septal wall. (F) Representative whole hearts for WT and RGS2^{eb} TG mice following 4 weeks of sham or TAC surgery. (G) Representative H&E staining of WT and RGS2^{eb} LV cross sections of WT and RGS2^{eb} TG cardiomyocytes following sham or TAC surgery. (H) Representative H&E staining of WT and RGS2^{eb} cardiomyocytes. Data represent means \pm SEM, $n = 6$ –13 per group. * $P < 0.05$, ** $P < 0.01$, and **** $P < 0.0001$ using two-way ANOVA with Bonferroni's *post hoc* test for multiple comparisons.

gene expression during cardiac hypertrophy is initially an adaptive process which increases the excitability, contractility, and plasticity of cardiac myocytes in response to pathological stress [40]. However, sustained fetal gene expression plays a causative role in maladaptive cardiac remodeling, leading to cardiac dysfunction and often the pathogenesis of heart failure [41]. In addition, our assessment of cardiac function obtained from pressure-volume loop analyses also suggests that RGS2^{eb} TG mice were able to maintain significantly improved cardiac function after TAC compared to WT mice, as evidenced by both systolic and diastolic indices (Fig. 3). Our data suggest that the expression of RGS2^{eb} appears to not only inhibit cardiac hypertrophy, but also

improves cardiac function without activation of fetal cardiac genes after 4 weeks of TAC, although the effect on fetal gene expression may more likely be due to an indirect effect of the inhibition of cardiac hypertrophy and apparent improvement in cardiac function, rather than a direct mechanistic connection between RGS2^{eb} and the re-expression of fetal genes. Further studies, such as prolonged exposure to TAC, may clarify the extent to which these effects are sustained.

Following transverse aortic constriction, RGS2 knockout mice have been found to develop severe cardiac hypertrophy and heart failure, as well as increased mortality compared to corresponding controls [15]. Although this clearly indicates that the presence of RGS2 is

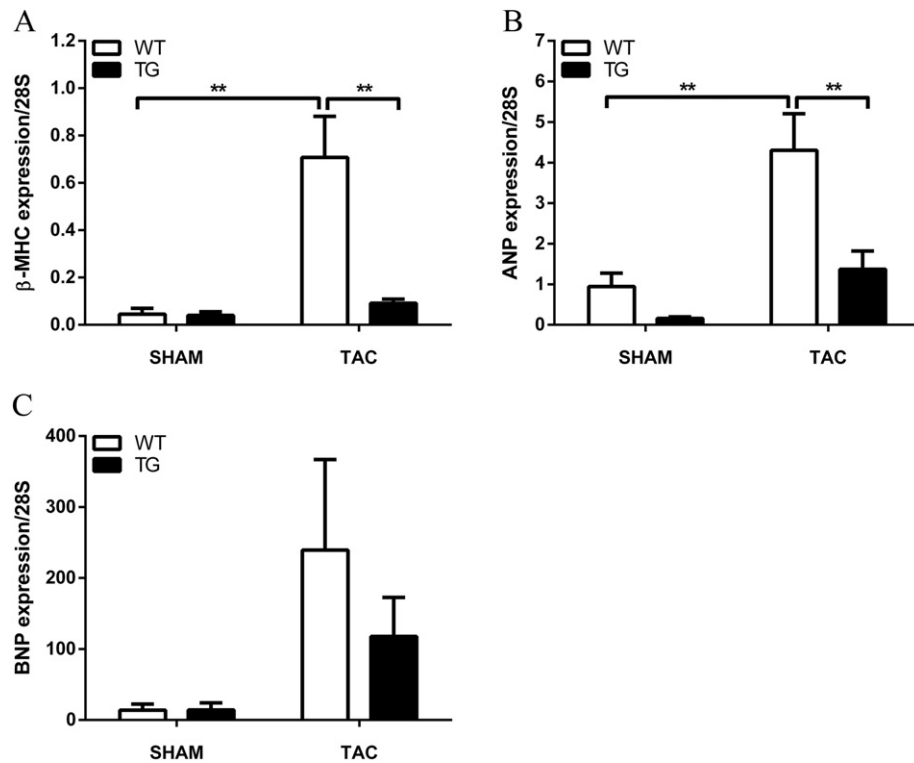


Fig. 5. Markers of cardiac hypertrophy. (A) β -MHC expression was significantly increased in WT TAC but not RGS2^{eb} TG mice after 4 weeks of aortic constriction. (B) ANP expression was also significantly elevated in WT TAC mice, while RGS2^{eb} TG mice maintained near-sham levels of expression. (C) BNP expression. Data represent means \pm SEM, n = 4–8 per group. * P < 0.05, ** P < 0.01, and *** P < 0.001 using two-way ANOVA with Bonferroni's *post hoc* test for multiple comparisons.

cardioprotective *in vivo*, many details of this beneficial effect remain to be elucidated [22]. In cultured ventricular myocytes, RGS2 is acutely and selectively upregulated in response to activators of G_q and G_s signaling [13,14,42]. However, RGS2 has been found to be ultimately downregulated *in vivo* following experimentally-induced hypertrophy and heart failure [29]. Furthermore, cardiac-specific overexpression of full-length RGS2 does not result in demonstrable cardioprotective effects in mice subjected to TAC [43]. Conversely, the overexpression of either RGS4, RGS5, or RGS10 has been shown to reduce cardiac hypertrophy [44–47], although it may be noted that unlike RGS2, these proteins tend to localize to the atria rather than the ventricles [46,48–51]. It is possible that the optimal level of RGS2 is decreased under conditions of hypertrophic stress, however a complete lack of RGS2 is clearly detrimental under pressure overload [15].

The lack of an observable protective effect of full-length RGS2 overexpression in the myocardium [43] stands in contrast to the present findings that expression of its isolated eIF2B-interacting domain (RGS2^{eb}) can protect against pathological cardiac hypertrophy and dysfunction *in vivo*. We have previously shown that the ability of RGS2^{eb} to inhibit drug-induced cell hypertrophy is independent of the G protein inhibitory effects of full-length RGS2 [22]. Along with our current findings, it follows that the RGS2^{eb} region may be an important contributor to the reported beneficial cardiac effects of RGS2. Since our previous studies suggest that the RGS2^{eb} region specifically binds to eIF2B and thereby inhibits protein synthesis [19], it is possible that some function of full length RGS2 may produce detrimental effects in the context of pathological hypertrophy, consistent with its observed downregulation in the latter condition [29]. Negative RGS2 effects could conceivably arise from its inhibition of beneficial G protein-mediated signals (e.g. the protective effects of adenosine) or alternatively *via* its effects on non-G protein targets such as tubulin or TRP channels [16,17]. To examine the importance of the RGS2^{eb} region *per se*, future studies would be in order, with expression of this truncated form targeted to the myocardium of full-body or cardiac-specific RGS2 knockout mice.

5. Conclusions

The present results suggest that expression of the eIF2B-interacting domain of RGS2, RGS2^{eb}, can protect against pathological cardiac hypertrophy and dysfunction *in vivo*, and that this may be *via* the direct inhibition of protein synthesis. We have previously shown the ability of RGS2^{eb} to inhibit drug-induced cardiomyocyte hypertrophy; along with our current findings, this suggests that the RGS2^{eb} region is an important contributor to the reported beneficial cardiac effects of RGS2.

Currently, the majority of drugs for cardiovascular diseases target GPCRs. Although these medications can offer significant benefits to patients, heart failure continues to be a global leading cause of morbidity and mortality. A better understanding of the various components that are part of the GPCR signalling pathways may lead to improved therapeutics, and interest in RGS2 and other RGS proteins as possible drug targets is on the rise [52–58]. In summary, this study has demonstrated that RGS2^{eb} is important in regulating *in vivo* cardiac hypertrophy and physiology, and suggests that this region of full-length RGS2 may be a key component of its reported cardioprotective effects.

Disclosures

The authors declare that they have no competing interests.

Acknowledgements

This work was supported and by a Grant In Aid (R2838A15, PC and QPF) and a Bridge Grant (7484, PC) from the Heart and Stroke Foundation of Ontario and an Operating Grant from the Canadian Institutes of Health Research (R2838A14, PC). PC and QPF were supported by Career Investigator Awards from the Heart and Stroke Foundation of Ontario. KNL was supported by an Ontario Graduate Scholarship.

References

- [1] D. Levy, R.J. Garrison, D.D. Savage, W.B. Kannel, W.P. Castelli, Prognostic implications of echocardiographically determined left ventricular mass in the Framingham Heart Study, *N. Engl. J. Med.* 322 (1990) 1561–1566.
- [2] K.T. Weber, C.G. Brilla, Pathological hypertrophy and cardiac interstitium. Fibrosis and renin-angiotensin-aldosterone system, *Circulation* 83 (1991) 1849–1865.
- [3] J. Heineke, J.D. Molkentin, Regulation of cardiac hypertrophy by intracellular signaling pathways, *Nat. Rev. Mol. Cell Biol.* 7 (2006) 589–600.
- [4] G.W. Dorn, T. Force, Protein kinase cascades in the regulation of cardiac hypertrophy, *J. Clin. Invest.* 115 (2005) 527–537.
- [5] M.C. Hendriks-Balk, S.L.M. Peters, M.C. Michel, A.E. Alewijnse, Regulation of G protein-coupled receptor signalling: Focus on the cardiovascular system and regulator of G protein signalling proteins, *Eur. J. Pharmacol.* 585 (2008) 278–291.
- [6] D.J. Campbell, A. Aggarwal, M. Esler, D. Kaye, Beta-blockers, angiotensin II, and ACE inhibitors in patients with heart failure, *Lancet (London, England)* 358 (2001) 1609–1610.
- [7] K. Chakir, W. Zhu, S. Tsang, A.Y.H. Woo, D. Yang, X. Wang, et al., RGS2 is a primary terminator of β -adrenergic receptor-mediated Gi signaling, *J. Mol. Cell. Cardiol.* 50 (2011) 1000–1007.
- [8] T. Anger, N. Klintworth, C. Stumpf, W.G. Daniel, U. Mende, C.D. Garlich, RGS protein specificity towards Gq- and Gi/o-mediated ERK 1/2 and Akt activation, *in vitro*, *J. Biochem. Mol. Biol.* 40 (2007) 899–910.
- [9] S.P. Heximer, S.P. Srinivasa, S. Bernstein, J.L. Bernard, E. Maurine, J.R. Hepler, et al., Cell biology and metabolism: G protein selectivity is a determinant of RGS2 function G protein selectivity is a determinant of RGS2 function*, *J. Biol. Chem.* 274 (1999) 34253–34259.
- [10] A.A. Roy, A. Baragli, L.S. Bernstein, J.R. Hepler, T.E. Hébert, P. Chidiac, RGS2 interacts with Gs and adenylyl cyclase in living cells, *Cell. Signal.* 18 (2006) 336–348.
- [11] S.P. Heximer, N. Watson, M.E. Linder, K.J. Blumer, J.R. Hepler, RGS2/G0S8 is a selective inhibitor of Gq α function, *Proc. Natl. Acad. Sci. U. S. A.* 94 (1997) 14389–14393.
- [12] A.A. Roy, C. Nunn, H. Ming, M.-X.X. Zou, J. Penninger, L.A. Kirshenbaum, et al., Up-regulation of endogenous RGS2 mediates cross-desensitization between Gs and Gq signaling in osteoblasts, *J. Biol. Chem.* 281 (2006) 32684–32693.
- [13] M.-X. Zou, A.A. Roy, Q. Zhao, L.A. Kirshenbaum, M. Karmazyn, P. Chidiac, RGS2 is up-regulated by and attenuates the hypertrophic effect of α 1-adrenergic activation in cultured ventricular myocytes, *Cell. Signal.* 18 (2006) 1655–1663.
- [14] C. Nunn, M.-X. Zou, A.J. Sobiesiak, A.A. Roy, L.A. Kirshenbaum, P. Chidiac, RGS2 inhibits β -adrenergic receptor-induced cardiomyocyte hypertrophy, *Cell. Signal.* 22 (2010) 1231–1239.
- [15] E. Takimoto, N. Koitabashi, S. Hsu, E.A. Ketner, M. Zhang, T. Nagayama, et al., Regulator of G protein signaling 2 mediates cardiac compensation to pressure overload and antihypertrophic effects of PDE5 inhibition in mice, *J. Clin. Invest.* 119 (2009) 408–420.
- [16] J.P. Schoeber, C.N. Topala, X. Wang, R.J. Diepens, T.T. Lambers, J.G. Hoenderop, et al., RGS2 inhibits the epithelial Ca²⁺ channel TRPV6, *J. Biol. Chem.* 281 (2006) 29669–29674.
- [17] K. Heo, S.H. Ha, Y.C. Chae, S. Lee, Y.-S. Oh, Y.-H. Kim, et al., RGS2 promotes formation of neurites by stimulating microtubule polymerization, *Cell. Signal.* 18 (2006) 2182–2192.
- [18] X. Wang, W. Zeng, A.A. Soyombo, W. Tang, E.M. Ross, A.P. Barnes, et al., Spinophilin regulates Ca²⁺ signalling by binding the N-terminal domain of RGS2 and the third intracellular loop of G-protein-coupled receptors, *Nat. Cell Biol.* 7 (2005) 405–411.
- [19] C.H. Nguyen, H. Ming, P. Zhao, L. Hugendubler, R. Gros, S.R. Kimball, et al., Translational control by RGS2, *J. Cell Biol.* 186 (2009) 755–765.
- [20] P. Anversa, A. Leri, M. Rota, T. Hosoda, C. Bearzi, K. Urbanek, et al., Concise review: stem cells, myocardial regeneration, and methodological artifacts, *Stem Cells* 25 (2007) 589–601.
- [21] A.B. Carvalho, Heart regeneration: Past, present and future, *World J. Cardiol.* 2 (2010) 107.
- [22] P. Chidiac, A.J. Sobiesiak, K.N. Lee, R. Gros, C.H. Nguyen, The eIF2B-interacting domain of RGS2 protects against GPCR agonist-induced hypertrophy in neonatal rat cardiomyocytes, *Cell. Signal.* 26 (2014) 1226–1234.
- [23] A. Subramaniam, W.K. Jones, J. Gulick, S. Wert, J. Neumann, J. Robbins, Tissue-specific regulation of the alpha-myosin heavy chain gene promoter in transgenic mice, *J. Biol. Chem.* 266 (1991) 24613–24620.
- [24] W.A. Kibbe, OligoCalc: an online oligonucleotide properties calculator, *Nucleic Acids Res.* 35 (2007) W43–W46.
- [25] H.A. Rockman, R.S. Ross, A.N. Harris, K.U. Knowlton, M.E. Steinhelper, L.J. Field, et al., Segregation of atrial-specific and inducible expression of an atrial natriuretic factor transgene in an *in vivo* murine model of cardiac hypertrophy, *Proc. Natl. Acad. Sci. U. S. A.* 88 (1991) 8277–8281.
- [26] S.A. Detombe, N.L. Ford, F. Xiang, X. Lu, Q. Feng, M. Drangova, Longitudinal follow-up of cardiac structure and functional changes in an infarct mouse model using retro-spectively gated micro-computed tomography, *Investig. Radiol.* 43 (2008) 520–529.
- [27] P. Pachter, T. Nagayama, P. Mukhopadhyay, S. Bátkai, D.A. Kass, Measurement of cardiac function using pressure-volume conductance catheter technique in mice and rats, *Nat. Protoc.* 3 (2008) 1422–1434.
- [28] S.A. Helms, G. Azhar, C. Zuo, S.A. Theus, A. Bartke, J.Y. Wei, Smaller cardiac cell size and reduced extra-cellular collagen might be beneficial for hearts of Ames dwarf mice, *Int. J. Biol. Sci.* 6 (2010) 475–490.
- [29] W. Zhang, T. Anger, J. Su, J. Hao, X. Xu, M. Zhu, et al., Selective loss of fine tuning of Gq/11 signaling by RGS2 protein exacerbates cardiomyocyte hypertrophy, *J. Biol. Chem.* 281 (2006) 5811–5820.
- [30] T. Scisense Inc, Understanding lusitropy: Passive diastolic properties and active myocardial relaxation, Scisense PV Tech. Note. (2017) 4–7.
- [31] P. Razeghi, M.E. Young, J.L. Alcorn, C.S. Moravec, O.H. Frazier, H. Taegtmeyer, Metabolic gene expression in fetal and failing human heart, *Circulation* 104 (2001) 2923–2931.
- [32] T.G. Parker, S.E. Packer, M.D. Schneider, Peptide growth factors can provoke “fetal” contractile protein gene expression in rat cardiac myocytes, *J. Clin. Invest.* 85 (1990) 507–514.
- [33] P.H. Sugden, J.F. Fuller, S.C. Weiss, A. Clerk, Glycogen synthase kinase 3 (GSK3) in the heart: a point of integration in hypertrophic signalling and a therapeutic target? A critical analysis, *Br. J. Pharmacol.* 153 (2009) S137–S153.
- [34] C.M. Abbott, C.G. Proud, Translation factors: in sickness and in health, *Trends Biochem. Sci.* 29 (2004) 25–31.
- [35] S.E. Hardt, H. Tomita, H.A. Katus, J. Sadoshima, Phosphorylation of eukaryotic translation initiation factor 2B ϵ by glycogen synthase kinase-3 β regulates β -adrenergic cardiac myocyte hypertrophy, *Circ. Res.* 94 (2004) 926–935.
- [36] G.I. Welsh, C.M. Miller, A.J. Loughlin, N.T. Price, Regulation of eukaryotic initiation factor eIF2B: glycogen synthase kinase-3 phosphorylates a conserved serine which undergoes dephosphorylation in response to insulin, *FEBS Lett.* 421 (1998) 125–130.
- [37] B.G. Petrich, Y. Wang, Stress-activated MAP kinases in cardiac remodeling and heart failure; new insights from transgenic studies, *Trends Cardiovasc. Med.* 14 (2004) 50–55.
- [38] J.D. Molkentin, G.W. Dorn, Cytoplasmic signaling pathways that regulate cardiac hypertrophy, *Annu. Rev. Physiol.* 63 (2001) 391–426.
- [39] N. Frey, E.N. Olson, Cardiac hypertrophy: The good, the bad, and the ugly, *Annu. Rev. Physiol.* 65 (2003) 45–79.
- [40] K. Kuwahara, T. Nishikimi, K. Nakao, Transcriptional regulation of the fetal cardiac gene program, *J. Pharmacol. Sci.* 119 (2012) 198–203.
- [41] S. Hannenhalli, M.E. Putt, J.M. Gilmore, J. Wang, M.S. Parmacek, J.A. Epstein, et al., Transcriptional genomics associates FOX transcription factors with human heart failure, *Circulation* 114 (2006) 1269–1276.
- [42] J. Hao, C. Michalek, W. Zhang, M. Zhu, X. Xu, U. Mende, Regulation of cardiomyocyte signaling by RGS proteins: Differential selectivity towards G proteins and susceptibility to regulation, *J. Mol. Cell. Cardiol.* 41 (2006) 51–61.
- [43] C. Park-Windhol, P. Zhang, M. Zhu, J. Su, L. Chaves, A.E. Maldonado, et al., Gq/11-mediated signaling and hypertrophy in mice with cardiac-specific transgenic expression of regulator of G-protein signaling 2, *PLoS One* 7 (2012) e40048.
- [44] J.H. Rogers, P. Tamirisa, A. Kovacs, C. Weinheimer, M. Courtois, K.J. Blumer, et al., RGS4 causes increased mortality and reduced cardiac hypertrophy in response to pressure overload, *J. Clin. Invest.* 104 (1999) 567–576.
- [45] H. Li, C. He, J. Feng, Y. Zhang, Q. Tang, Z. Bian, et al., Regulator of G protein signaling 5 protects against cardiac hypertrophy and fibrosis during biomechanical stress of pressure overload, *Proc. Natl. Acad. Sci. U. S. A.* 107 (2010) 13818–13823.
- [46] R. Miao, Y. Lu, X. Xing, Y. Li, Z. Huang, H. Zhong, et al., Regulator of G-protein signaling 10 negatively regulates cardiac remodeling by blocking mitogen-activated protein kinase-extracellular signal-regulated protein kinase 1/2 signaling, *Hypertension* 67 (2016) 86–98.
- [47] J.H. Rogers, A. Tsirka, A. Kovacs, K.J. Blumer, G.W. Dorn, A.J. Muslin, RGS4 reduces contractile dysfunction and hypertrophic gene induction in Galpha q overexpressing mice, *J. Mol. Cell. Cardiol.* 33 (2001) 209–218.
- [48] C. Mittmann, C.H. Chung, G. Höppner, C. Michalek, M. Nose, C. Schüler, et al., Expression of ten RGS proteins in human myocardium: Functional characterization of an upregulation of RGS4 in heart failure, *Cardiovasc. Res.* 55 (2002) 778–786.
- [49] C. Larmine, P. Murdock, J.-P. Walhin, M. Duckworth, K.J. Blumer, M.A. Scheideler, et al., Selective expression of regulators of G-protein signaling (RGS) in the human central nervous system, *Mol. Brain Res.* 122 (2004) 24–34.
- [50] S. Gu, C. Cifelli, S. Wang, S.P. Heximer, RGS proteins: identifying new GAPs in the understanding of blood pressure regulation and cardiovascular function, *Clin. Sci. (Lond.)* 116 (2009) 391–399.
- [51] C.A. Doupnik, T. Xu, J.M. Shinaman, Profile of RGS expression in single rat atrial myocytes, *Biochim. Biophys. Acta-Gene Struct. Expr.* 1522 (2001) 97–107.
- [52] B. Sjögren, S. Parra, L.J. Heath, K.B. Atkins, Z. Xie, R. Neubig, Cardiotonic steroids stabilize RGS2 protein levels, *Mol. Pharmacol.* (2012) (mol.112.079293).
- [53] B. Sjögren, R.R. Neubig, Thinking outside of the “RGS box”: New approaches to therapeutic targeting of regulators of G protein signaling, *Mol. Pharmacol.* 78 (2010) 550–557.
- [54] B. Sjögren, L.L. Blazer, R.R. Neubig, Regulators of G protein signaling proteins as targets for drug discovery, *Prog. Mol. Biol. Transl. Sci.* 91 (2010) 81–119.
- [55] T.H. Le, T.M. Coffman, RGS2: a “turn-off” in hypertension, *J. Clin. Invest.* 111 (2003) 441–443.
- [56] A.S. Go, D. Mozaffarian, V.L. Roger, E.J. Benjamin, J.D. Berry, W.B. Borden, et al., Heart disease and stroke statistics—2013 update a report from the American Heart Association, *Circulation* 127 (2013) e6–e245.
- [57] E.M. Turner, L.L. Blazer, R.R. Neubig, S.M. Husbands, Small molecule inhibitors of regulator of G protein signalling (RGS) proteins, *ACS Med. Chem. Lett.* 3 (2012) 146–150.
- [58] B. Sjögren, S. Parra, K.B. Atkins, B. Karaj, R.R. Neubig, B. Sjögren, et al., Digoxin-mediated up-regulation of RGS2 protein protects against cardiac injury, *J. Pharmacol. Exp. Ther.* (2016) 357.